THE JOURNAL OF NAVIGATION (2018), **71**, 299–316.
doi:10.1017/S0373463317000698

A New Indoor Positioning System Using Artificial Encoded Magnetic Fields

Falin Wu, Yuan Liang, Yong Fu and Chenghao Geng

(School of Instrumentation Science and Opto-electronics Engineering, Beihang University, Beijing, China)
(E-mail: liangyuan@buaa.edu.cn)

The demand for accurate indoor positioning continues to grow but the predominant positioning technologies such as Global Navigation Satellite Systems (GNSS) are not suitable for indoor environments due to multipath effects and Non-Line-Of-Sight (NLOS) conditions. This paper presents a new indoor positioning system using artificial encoded magnetic fields, which has good properties for NLOS conditions and fewer multipath effects. The encoded magnetic fields are generated by multiple beacons; each beacon periodically generates unique magnetic field sequences, which consist of a gold code sequence and a beacon location sequence. The position of an object can be determined with measurements from a tri-axial magnetometer using a three-step method: performing time synchronisation between sensor and beacons, identifying the beacon field and the beacon location, and estimating the position of the object. The results of the simulation and experiment show that the proposed system is capable of achieving Two-Dimensional (2D) and Three-Dimensional (3D) accuracy at sub-decimetre and decimetre levels, respectively.

KEYWORDS

1. Indoor positioning. 2. Magnetic field. 3. Magnetometer.

Submitted: 7 October 2016. Accepted: 23 August 2017. First published online: 11 October 2017.

1. INTRODUCTION. Navigation and positioning are necessary functions for modern human life, and many technologies have been developed, such as Global Navigation Satellite Systems (GNSS), which are widely applied in outdoor environments since they provide convenient and reliable results. However, there is no reliable universal method for indoor environments due to the effects of multipath, signal attenuations and Non-Line-Of-Sight (NLOS) conditions. Recently, there has been a growing interest in positioning systems using magnetic fields. A magnetic field has the desirable properties of penetrating common building materials and being resistant to multipath effects (Pasku et al., 2015). In addition, the popularity of portable devices equipped with magnetic sensors promotes the research of magnetic field applications. Generally, a positioning system using a magnetic field mainly employs the following sources: the Earth's magnetic field; electromagnetic fields; and artificial magnetic fields.

Artificial magnetic fields can be generated by a permanent magnet and current coil. The position of an object can be determined by using the strength and the direction of the magnetic field. The available range of a permanent magnet field is limited, and therefore, this method is mostly used in medical applications (Hu et al., 2010; Song et al., 2009). Current coils can generate a quasi-static magnetic field through a pulsed Direct Current (DC) or an Alternating Current (AC) with low frequency. Blankenbach and Norrdine (2010) describe a DC artificial magnetic field for indoor positioning. In order to distinguish different magnetic field components of multiple coils, a Time Division Multiple Access (TDMA) approach was used. The interference of DC components and high-frequency noise components in the signal can be filtered by calculating the difference of the measured magnetic field caused by switching DC and a digital Finite Impulse Response (FIR), respectively. However, the time synchronisation between the magnetic sensor and the coils' signal requires high accuracy when the number of distributed coils increases. Sheinker et al. (2013a; 2013b) introduced a Two-Dimensional (2D) and Three-Dimensional (3D) localisation system using multiple beacons using AC. The frequency of the magnetic field is in the Ultra-Low Frequency (ULF) band (0·3-3 kHz) which allows deeper penetration. The magnetic field, amplitude, and phase of different beacons can be deduced by a different model and corresponding lock-in amplifiers with a phase recovery block. While using a Frequency Division Multiple Access (FDMA) approach certainly requires more lock-in amplifiers, the frequency assigned to each beacon is definitely higher if the number of beacons increases. Prigge and How (2004) presented a magnetic field positioning system using Code Division Multiple Access (CMDA), and they analysed the performance of three signal structures, i.e., TDMA, FDMA, and CDMA. Each signal structure performs well when using a small number of beacons. The CMDA structure enables a large number of beacons to keep a good performance compared with other structures, since it does not cause the beacon signal frequency to move higher.

In this paper, the encoded magnetic fields of multiple beacons are applied to an indoor positioning system. The sequence of each beacon field consists of a Gold code and the sequence of the beacon location. The Gold code has the desirable properties of autocorrelation and cross-correlation (Misra and Enge, 2006) in the CDMA structure, which can not only implement time synchronisation between a mobile device and beacons, but can also distinguish between the different magnetic fields. Therefore, the proposed system does not require a communication link to complete time synchronisation. In addition, the mobile device does not need to know the beacon location before positioning. These advantages make the system more practicable, especially for different buildings.

The rest of this paper is organised as follows. Firstly, the magnetic field of the beacon is described in Section 2. Then, the positioning algorithms and proposed system are introduced in Section 3. The simulation and the test of system performance are presented in Section 4 and Section 5, respectively. Finally, Section 6 summarises our conclusions and outlines future work.

2. SYSTEM DESIGN.

2.1. *Magnetic field of beacon.* Each beacon consists of numerous current carrying coils to generate a magnetic field. According to the Biot-Savart law (Reitz et al., 2008), the magnetic field at a point $P(x, y, z)$ generated by current carrying circular loops with n turns,

https://doi.org/10.1017/S0373463317000698 Published online by Cambridge University Press

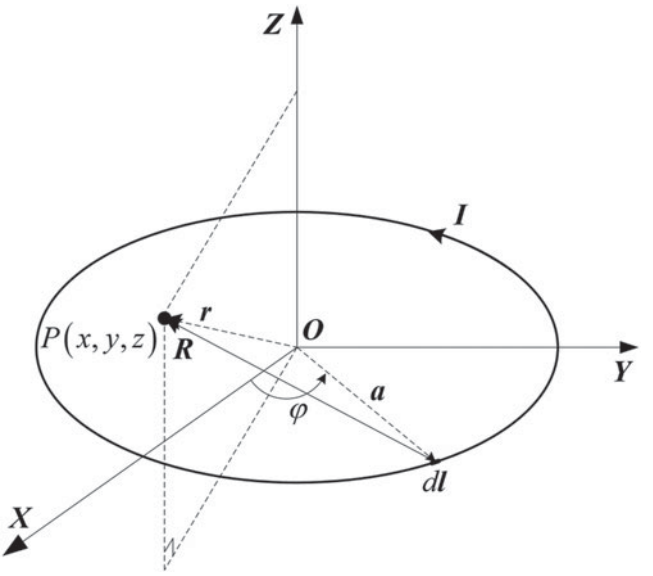

Figure 1. The circular coils with radius a and n turns are located in the centre of the Cartesian coordinates.

as shown in Figure 1, is given by

$$\boldsymbol{B} = \frac{n\mu_0}{4\pi}\oint \frac{I d\boldsymbol{l} \times \boldsymbol{R}}{R^3} \tag{1}$$

where $\boldsymbol{B}$ is the magnetic flux density and $\mu_0 = 4\pi \times 10^{-3}$ G m/A is the permeability of a vacuum. $\boldsymbol{I}$ is the current flowing through the coils, $d\boldsymbol{l}$ is the differential length of the current carrying coils and $\boldsymbol{R} = \boldsymbol{r} - \boldsymbol{a}$ is the distance vector from $d\boldsymbol{l}$ to the point P. $\boldsymbol{a}$ is the radius of the current carrying coils, φ is the angle between the x-axis and the vector of $Id\boldsymbol{l}$, as illustrated in Figure 1 and $d\boldsymbol{l}$ is derived by

$$d\boldsymbol{l} = -a\sin\varphi d\varphi \boldsymbol{i} + a\cos\varphi d\varphi \boldsymbol{j} \tag{2}$$

where $\boldsymbol{i}$ and $\boldsymbol{j}$ are the unit vectors along x-axis and y-axis, respectively. The distance vector $\boldsymbol{R}$ can be calculated by

$$\boldsymbol{R} = (x - a\cos\varphi)\boldsymbol{i} + (y - a\sin\varphi)\boldsymbol{j} + z\boldsymbol{k} \tag{3}$$

where $\boldsymbol{k}$ is the unit vector along the z-axis. If $r \gg a$, the magnetic field created by the coils can be represented by a magnetic dipole as the far-field model, and therefore $\boldsymbol{B}$ can be written simply as

$$B_x = \frac{3\mu_0 nIa^2 xz}{4r^5} \tag{4}$$

$$B_y = \frac{3\mu_0 nIa^2 yz}{4r^5} \tag{5}$$

$$B_z = \frac{\mu_0 nIa^2\left(2z^2 - x^2 - y^2\right)}{4r^5} \tag{6}$$

https://doi.org/10.1017/S0373463317000698 Published online by Cambridge University Press

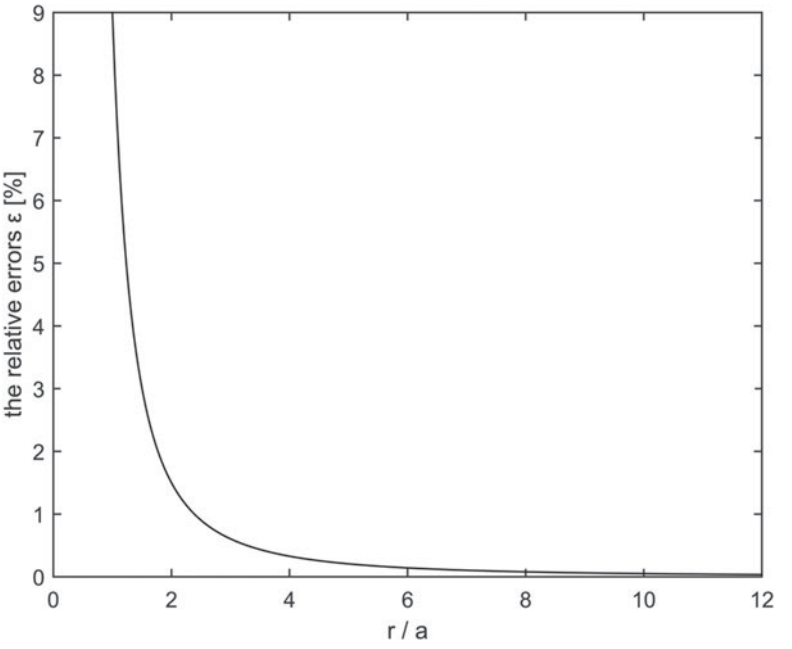

Figure 2. The relative errors of between the theoretical model and far-field model.

where $r = \sqrt{x^2 + y^2 + z^2}$. The relative errors between theoretical model and far-field model are given by

$$\varepsilon = \frac{|\boldsymbol{B}_{the} - \boldsymbol{B}_{far}|}{|\boldsymbol{B}_{the}|} \times 100\% \tag{7}$$

where $\boldsymbol{B}_{the}$ is obtained by using the theoretical model and $\boldsymbol{B}_{far}$ is calculated by using a far-field model. Figure 2 depicts the relative error between the theoretical model and far-field model. The location of coils is $(0, 0, 0)$, the number of turns is $n = 100$, current flowing through coil is $I = 3$ A, radius of the loop is $a = 0{\cdot}25$ m, the object is located at point $(0, 0, z)$, and z varies from $0{\cdot}25$ m to 3 m. From the curves, it can be inferred that a large magnetic field error may exist when using the far-field model at close range.

2.2. *The Beacon Configuration.* The available range of beacon field created by current carrying coils is limited due to the attenuation characteristics of magnetic fields which obviously decreases with distance. For the purpose of enlarging the coverage area of the beacon field, the magnitude of magnetic dipole moment $\boldsymbol{M}$ should be large, and the configuration of the beacon should be appropriate, especially for a large building. Owing to $|\boldsymbol{M}| = nI\pi a^2$, $|\boldsymbol{M}|$ can be increased through increasing the loop current $\boldsymbol{I}$, the number of turns n, or the radius of coils a. However, due to the limitation of interior space and cost, it is impractical to use a large size for the beacon with many coils and, in particular, superconducting coils producing a high current (Kong et al., 2004). Thus, multiple beacons are required to provide a magnetic field signal for a large indoor space. The effective range of the magnetic field generated by the same size beacon is approximately the same, regardless of whether the beacon is composed of uniaxial coils (Prigge and How, 2004), biaxial coils (Bernieri et al., 2013) and triaxial coils (Abrudan et al., 2015). Uniaxial coils have

https://doi.org/10.1017/S0373463317000698 Published online by Cambridge University Press

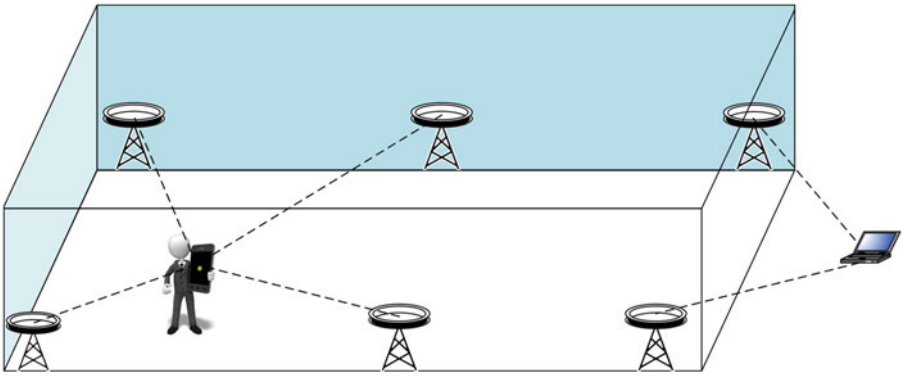

Figure 3. The positioning system using encoded magnetic fields generated by multiple magnetic beacons; each beacon is assigned a unique Gold code and a location sequence to form an integrated magnetic field sequence.

more advantages over multi-axis coils in terms of manufacturing and model complexity. In addition, an extra computational load is certainly required if uniaxial beacons are oriented in different directions. Consequently, uniaxial coils are employed as beacons in this paper, and each beacon is fixed and coplanar in the indoor environment.

The distance between beacons depends on the resolution of the object's three-axis magnetometer. A high resolution sensor such as HMR2300r (Blankenbach et al., 2012) is able to measure the weak magnetic field signal, which can increase the distance between beacons and decrease the number of beacons.

2.3. *Encoded Magnetic Fields.* The integrated encoded magnetic field sequences of each beacon consists of a unique Gold code and its location sequence; the location sequence is represented as a binary code according to the location coordinates of the beacon, which is modulated onto the end of the Gold code sequence with binary encoding. In the integrated sequence, 1 and 0 represent the forward and reverse current, respectively. All beacons periodically create encoded magnetic fields at the same time so that the process of synchronisation and location solution can be performed. Although the synchronisation between sensor and beacon can be rapidly implemented by means of wired or wireless communication, the Gold code sequence has not lived up to its full potential in this way. In addition, this will probably increase the cost of beacons. All beacon locations can be stored in portable devices before positioning, whereas once one beacon location has been changed or placed in a new building (with the assumption that the location database has not been updated), the positioning method cannot work. For a positioning system using encoded magnetic fields, as long as the Gold code sequence is much longer than the location sequence, the time synchronisation can be implemented based on the desirable correlation property of the Gold code sequence, and thus the Gold code and location sequence can be distinguished. This means that the portable device only needs to store Gold code sequences.

The positioning system is shown in Figure 3, the computer assigns a unique Gold code and location sequence to each beacon distributed in the indoor environment so as to generate superposed encoded magnetic fields; the object uses a three-axis magnetometer to measure the superposition fields around beacons. The position of an object can be determined in three steps: first, performing time synchronisation between sensor and beacons;

https://doi.org/10.1017/S0373463317000698 Published online by Cambridge University Press

second, identifying the beacon field and the beacon location; third, estimating the position of the object.

3. POSITIONING ALGORITHMS.

3.1. *Time Synchronisation.* An integrated, encoded magnetic field sequence of the i-th beacon, designated as S_i, consists of a Gold code gs_i and its location sequence ls_i, i.e., the integrated sequence is composed of the number 1 or -1, which represents the direction of current. Since orthogonal Gold codes have a good performance for autocorrelation and cross-correlation, the time synchronisation between the beacons and the sensor can be implemented by performing correlation detection when the length of gs_i is much longer than ls_i. The correlation function is defined by Pursley (1977) as

$$cor(j) = \frac{1}{T}\sum_{k=1}^{T} S_i(k-j)gs_i(k) \tag{8}$$

where $cor(j)$ is the correlation value of the j-th bit of S_i and T is the length of gs_i. If the sequence in S_i matches with gs_i, the peak of the correlation value, which is consistent with the initial position of the periodical encoded magnetic field sequence, can be found. Consequently, the synchronisation is completed by using the peak point.

For the measurement sequence of superposed encoded magnetic fields, ***MS***, the correlation detection utilises the phase of ***MS***. To extract the initial position of the encoded magnetic sequence from the measurement sequence, the correlation value $cor(j)$ can be rewritten as

$$cor(j) = \frac{1}{T}\sum_{k=1}^{T} MP_i(k-j)gs_i(k) \tag{9}$$

where MP_i is the i-th phase of ***MS*** and is either 1 or -1. The peak of cor is unlikely to be the same value as the result of Equation (8) unless the object is near a certain beacon such that the beacon field masks another beacon field, since received signal strength decreases rapidly with increasing distance.

As to three directions of the measurement sequences of a three-axis magnetometer, $\boldsymbol{MS}_w(w = x, y, z)$, the results of correlation detection are probably not as good as they could be, especially when the object is around the centre of multiple beacons or at some locations in the symmetrical magnetic field. Correlation curves are likely to appear with more than one equal peak at different time nodes. Therefore, a regulation for distinguishing the initial position of the superposed, encoded magnetic field sequence is required for synchronisation when using measurements of the three-axis magnetometer. In this paper, the peak value of the correlation detection is compared with a threshold 0·6, which is obtained from simulation and experiments. If one or more correlation detections of three direction measurements appear, with only one peak at the same time in a period and the absolute value of peak is higher than 0·6, the time node at which peak appears can be considered as the mark of time synchronisation. In this case, the result reveals that the location of the object is near one of beacons, and thus, the correlation detection has good performance. If none of the absolute values of the peaks are higher than 0·6, the location of the object is likely to be near the centre of multiple beacons, and the correlation detection among three direction measurements might give some unsatisfactory results. For example, the correlation detection of a

https://doi.org/10.1017/S0373463317000698 Published online by Cambridge University Press

certain direction measurement appears in more than one of the same magnitude peaks at different times in a period, or the correlation detection of different direction measurements peak at different times. Even so, the time node, which peaks most times among different direction correlation detections, can be treated as the mark of time synchronisation.

3.2. *Beacon Field Estimation and Beacon Location Demodulation.* The total number of beacons is designated as h. Assuming that the Earth's magnetic field is constant and b_w describes its constant bias along the w axis, the theoretical value of $\boldsymbol{MS}_w, \boldsymbol{MS}_{tw}$, can be calculated by using the following equation (Prigge, 2004)

$$\boldsymbol{MS}_{tw} = \sum_{i=1}^{T+l} B_{iw} S_i + b_w \tag{10}$$

where B_{iw} is the magnetic field produced by beacon i along the w axis, and l is the length of ls_i. The matrix form of Equation (10) can be expressed as

$$\boldsymbol{MS}_{tw} = \boldsymbol{A}\boldsymbol{X}_w, \tag{11}$$

where $\boldsymbol{MS}_{tw} = [ms_w(1)\ ms_w(2)\ ms_w(3)\ \cdots\ ms_w(T+l)]^T$, $\boldsymbol{X}_w = [B_{1w}\ B_{2w}\ B_{3w}\ \cdots\ B_{hw}\ b_w]^T$ is $(h+1) \times 1$ sequence, $\boldsymbol{A}$ is $(T+l) \times (h+1)$ matrix:

$$\boldsymbol{A} = \begin{bmatrix} s_1(1) & s_2(1) & s_3(1) & \cdots & s_h(1) & 1 \\ s_1(2) & s_2(2) & s_3(2) & \cdots & s_h(2) & 1 \\ s_1(3) & s_2(3) & s_3(3) & \cdots & s_h(3) & 1 \\ \vdots & \vdots & \vdots & \ddots & \vdots & 1 \\ s_1(T+l) & s_2(T+l) & s_3(T+l) & \cdots & s_h(T+l) & 1 \end{bmatrix} \tag{12}$$

where $s_j(i)(j = 1, 2, 3, \cdots, h)$ is the i-th element of S_j. The estimation of $\boldsymbol{X}_w$, designated $\boldsymbol{X}_{ew}$, can be derived from least squares fit after time synchronisation

$$\boldsymbol{X}_{ew} = \left(\boldsymbol{A}_G^T \boldsymbol{A}_G\right)^{-1} \boldsymbol{A}_G^T \boldsymbol{MS}_{Gw} \tag{13}$$

where $\boldsymbol{MS}_{Gw}$ is the first T bit of $\boldsymbol{MS}_w$, $\boldsymbol{A}_G$ is the matrix consisting of Gold codes and constant 1:

$$\boldsymbol{A}_G = \begin{bmatrix} s_1(1) & s_2(1) & s_3(1) & \cdots & s_h(1) & 1 \\ s_1(2) & s_2(2) & s_3(2) & \cdots & s_h(2) & 1 \\ s_1(3) & s_2(3) & s_3(3) & \cdots & s_h(3) & 1 \\ \vdots & \vdots & \vdots & \ddots & \vdots & 1 \\ s_1(T) & s_2(T) & s_3(T) & \cdots & s_h(T) & 1 \end{bmatrix} \tag{14}$$

To take full advantage of each beacon field, the maximum measurable range of the sensor for the beacon field, mr, can be set as the distance between beacons according to the

https://doi.org/10.1017/S0373463317000698 Published online by Cambridge University Press

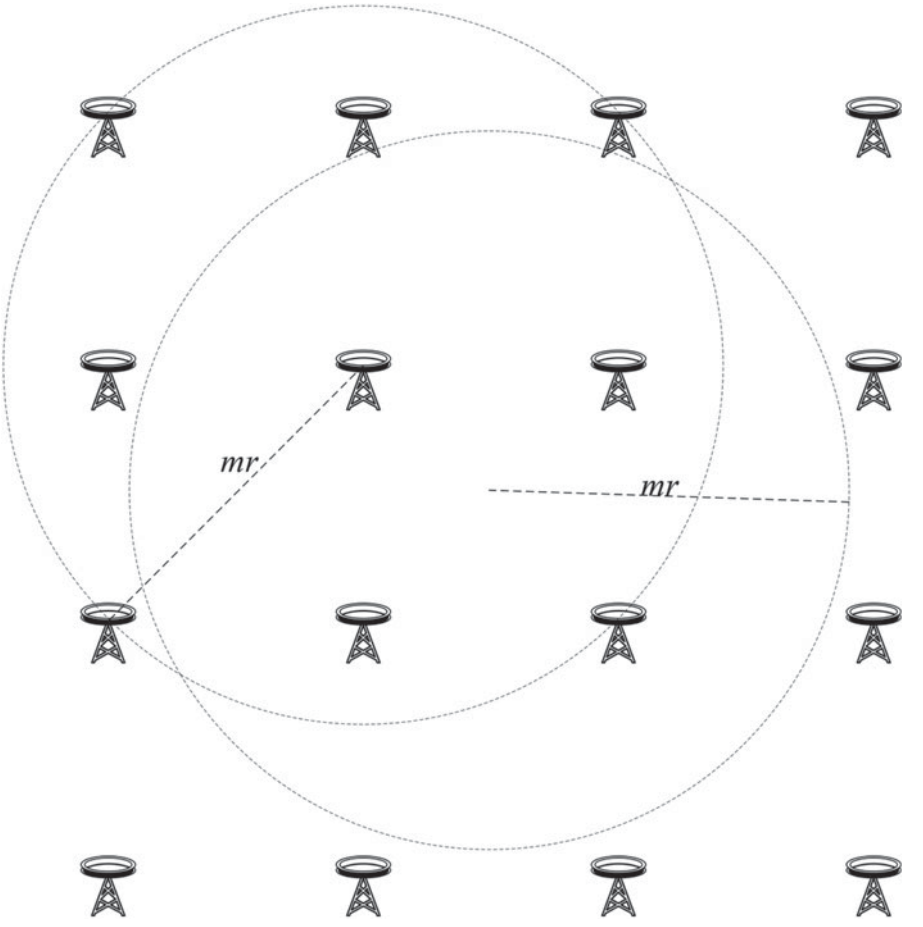

Figure 4. The distance between beacons is related to the measurable range of the sensor, which results in limited beacon field contribution to the measurements.

above analysis of the beacon configuration. Therefore, the three-axis magnetometer can measure only four to nine beacon fields since the beacon field attenuates rapidly with the increase of distance r, as shown in Figure 4. These effective beacon fields can be deduced from the results of beacon field estimation. An obvious characteristic, theoretically, is the magnitude that these beacon fields are higher than other beacons. The number of beacon locations required to be estimated can be divided into two possible scenarios: the first, is that the maximum estimation beacon field is much higher than other beacon fields, which means that the object is near a certain beacon and the number of usable beacon locations is higher than four; the second is the first four maximum magnitudes of the beacon fields do not appear to be much different, which means that the object is near the centre of multiple beacons, and thus the positioning estimation of the object requires only four beacon locations.

Since the number of effective beacons is limited, and each bit of the beacon location sequence is composed of a 1 or -1, the combinations of beacon location sequence are

https://doi.org/10.1017/S0373463317000698 Published online by Cambridge University Press

confined. The combinations of usable beacon location sequence can be calculated by

$$\begin{bmatrix} L_w(1) \\ L_w(2) \\ L_w(3) \\ \vdots \\ L_w(2^{eh}) \end{bmatrix} = \begin{bmatrix} -1 & -1 & -1 & \cdots & -1 & 1 \\ 1 & -1 & -1 & \cdots & -1 & 1 \\ -1 & 1 & -1 & \cdots & -1 & 1 \\ \vdots & \vdots & \vdots & \ddots & \vdots & 1 \\ 1 & 1 & 1 & \cdots & 1 & 1 \end{bmatrix} \begin{bmatrix} B_{ew}(1) \\ B_{ew}(2) \\ B_{ew}(3) \\ \vdots \\ B_{ew}(eh) \\ b_w \end{bmatrix} \tag{15}$$

where eh is the number of usable beacon location sequences and $L_{gw}(i)(i = 1, \cdots, 2^{eh})$ is the possible value of superposed magnetic field sequence based on beacon location sequence. $B_{ew}(j)(j = 1, \cdots, eh)$ is the magnitude of the effective beacon field. The matrix comprised of 1 or -1 is the possible combination of the beacon location sequences. The real combination of magnetic field sequence can be deduced by the minimum deviation between measurement and possible combination value

$$\min |L_w(i) - ms_w(g)|, \quad i = 1, 2, \cdots, 2^{eh} \tag{16}$$

where $ms_w(g), (g = T, T + 1, \cdots, T + l)$ is the magnetic field measurement of the beacon location sequence part. The mode of three axes results is the real combination. The function of the minimum deviation is to make a reliable estimated combination matched with the real combination. Each bit of the real combination can be deduced successively from the minimum deviation, and the binary beacon location sequence can be obtained after transforming -1 to 0, thus, effective beacon locations are known to the object.

3.3. *Position Determination.* After beacon field estimation and beacon location demodulation, the 3D positon of the object, (x, y, z), can be determined based directly on the far-field model if the object is near the centre of multiple beacons. The magnetic field generated by the i-th beacon at the object, in the beacons' fixed coordinate frame, can be represented as follows:

$$\begin{cases} B_{ix} = \dfrac{3\mu_0 NIS\,(x - x_i)\,(z - z_i)}{4\pi r_i^5} \\ B_{iy} = \dfrac{3\mu_0 NIS\,(y - y_i)\,(z - z_i)}{4\pi r_i^5} \\ B_{iz} = \dfrac{\mu_0 NIS\left[2\,(z - z_i)^2 - (x - x_i)^2 - (y - y_i)^2\right]}{4\pi r_i^5} \end{cases} \tag{17}$$

where B_{ix}, B_{iy} and B_{iz} are the components of the magnetic field along the x, y and z axis, respectively. (x_i, y_i, z_i) is the location of the i-th beacon, $r_i = \sqrt{(x - x_i)^2 + (y - y_i)^2 + (z - z_i)^2}$ is the distance from the object to the i-th beacon and $S = \pi a^2$ is the area of the coils. The magnitude of $\boldsymbol{B}_i$ can be calculated by

$$|\boldsymbol{B}_i| = \sqrt{B_{ix}^2 + B_{iy}^2 + B_{iz}^2} = \sqrt{B_{ex}^2(i) + B_{ey}^2(i) + B_{ez}^2(i)} \tag{18}$$

On the basis of the effective beacon location (x_i, y_i, z_i), Equation (18) can be equivalently rewritten as

$$|\boldsymbol{B}_i| = \frac{\mu_0 NIS}{4\pi r_i^4}\sqrt{3(z - z_i)^2 + r_i^2} \tag{19}$$

https://doi.org/10.1017/S0373463317000698 Published online by Cambridge University Press

The position of the object can be estimated by using the Gauss-Newton method or the Levenberg-Marquardt (LM) algorithm to solve Equation (19), since the Gauss-Newton method is sensitive to the initial value, i.e., the initial position estimation of the object is required to be close to the solution. The approximate value of the initial value can be deduced by (Prigge and How, 2004):

$$|\boldsymbol{B}_i| \approx \frac{1{\cdot}5\mu_0 NIS}{4\pi r_i^3} \tag{20}$$

The attitude of the object can be estimated as well after the position has been obtained. Since the sensor coordinate frame may not be consistent with the beacons' fixed coordinate frame, there is a transformation relation between the direction cosine matrix between the measurements of the three-axis magnetometer $\boldsymbol{MS}_w$ and the theoretical value $\boldsymbol{MS}_{tw}$. Consequently, the beacon field along the three directions in the beacons' fixed coordinate frame, (B_{ix}, B_{iy}, B_{iz}), can be transformed into the estimation $(B_{ex}(i), B_{ey}(i), B_{ez}(i))$ based on the direction cosine matrix $\boldsymbol{C}$

$$\begin{bmatrix} B_{ex}(i) \\ B_{ey}(i) \\ B_{ez}(i) \end{bmatrix} = \boldsymbol{C} \begin{bmatrix} B_{ix} \\ B_{iy} \\ B_{iz} \end{bmatrix} \tag{21}$$

The direction cosine matrix contains attitude information of the object described by three Euler angles, and it can be deduced by the singular value decomposition method (Markley, 1987). If the coordinate frames of the sensor and beacons are consistent, Equation (17) can be applied to directly determine the position of the object. The three direction measurements provide additional information to ensure the reliability of positioning, especially when the magnitude of the Earth's magnetic field or interference is so large that it masks the measurement along a certain axis. Other direction data are still available for positioning.

For the scenario that the object is near a certain beacon, most of the magnetometer measurements come from the magnetic field created by this beacon. According to the above analysis of beacon magnetic field distribution, the positioning results based on the far-field for this scenario may result in some errors, since the real installation is inaccurate when compared to a theoretical model. A straightforward solution is using all the usable beacon fields which are much stronger than other beacons except for the maximum beacon field, so that the far-field model is available.

4. SIMULATION OF POSITIONING METHOD. In order to verify the proposed positioning method using encoded magnetic fields, a simulation is performed. 16 beacons are fixed in an indoor space of $12 \times 12 \times 4\,\mathrm{m}^3$ to generate encoded magnetic fields where each beacon is comprised of circular coils with 100 turns and the radius of the coils is 0·25 m. The current flowing in the coils is 3 A, and its polarity is switched according to the assigned sequence. The location of each beacon and the unique sequence assigned to them are shown in Table 1. The length of each Gold code sequence is 127, and all of them are represented as a hexadecimal number in Table 1. The location sequence is represented as a binary code according to their location coordinates. The whole sequence is composed of a Gold code and location sequence, and its length is 139. '1' and '0' represent positive current and negative current respectively. Each beacon periodically generates a magnetic field at the same time according to the assigned sequence, and the update rate of each sequence is 1 Hz. We

https://doi.org/10.1017/S0373463317000698 Published online by Cambridge University Press

Table 1. The Configuration of Beacons.

Beacon Number	Location	Encoded Magnetic Field Sequence	
		Gold code sequence	Location sequence
1	(0, 0, 0)	0B70E25ADDB7CE91CCC9B8558F35C04	000000000000
2	(4, 0, 0)	0DA7A41ED483399E2F78F3BF0A89252	010000000000
3	(8, 0, 0)	4F79D6ADD2547FDA264C04B0E9386EC	100000000000
4	(12, 0, 0)	87F8F03333A809F35B1CB32C45F9DB1	110000000000
5	(0, 4, 0)	4BE3AD2A238CDA2F64927603EFEF288	000001000000
6	(4, 4, 0)	2DEE03A6AB9EB3C17B5514943AE4514	010001000000
7	(8, 4, 0)	3DCAD07A941076EED143E701A2D2EB7	100001000000
8	(12, 4, 0)	16FABD0EF050E5A1A1BDDC151C7AB0B	110001000000
9	(0, 8, 0)	49AE90E9DB6088D5C5FD4F5A6C848BA	000010000000
10	(4, 8, 0)	ACC89D4757E89ABC2BE28838FB5180D	010010000000
11	(8, 8, 0)	DE7B9B9011AC9388DCED6B89B0BB056	100010000000
12	(12, 8, 0)	E72218FBB28E9712A76A9A51154E47B	110010000000
13	(0, 12, 0)	B5D8B9948BD7147904489ECB6EC9B66	000011000000
14	(4, 12, 0)	6449BBD9B614EC9556B23FA45790350	010011000000
15	(8, 12, 0)	BA3B08DF6152A89C62453047E6DBDF8	100011000000
16	(12, 12, 0)	D502515C0AF18A98F83EB7B63E7E2AC	110011000000

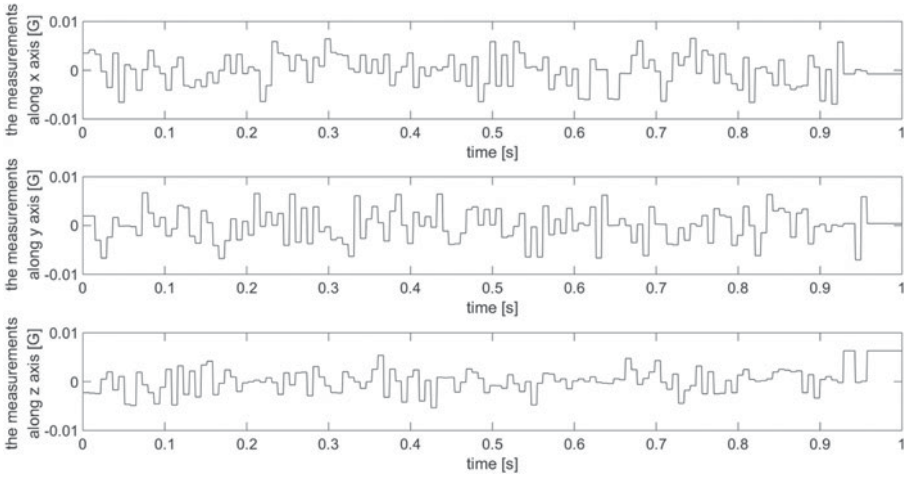

Figure 5. The encoded magnetic fields measurement along x, y, and z axes.

assume that the magnitude of the geomagnetic field is zero, and the sensor frame coincides with the beacon reference frame. If the sample rate of sensor is 2,000 Hz, and the location of the object is (5·8, 6·1, 1·2), the three axes measurements of encoded magnetic fields at the location of the object in one second are shown in Figure 5.

Although the measurements are apparently the sum of each beacon's encoded magnetic fields, the beacon field is too weak to measure for the long distance beacons. Consequently, only those beacons that are near the object can be used for time synchronisation, and the successful sign for synchronisation is the appearance of larger peaks during the correlation detection process. Figure 6 shows the following: the correlation detection of four beacons near the object, three peaks along three orthogonal axes appear at the same time point,

https://doi.org/10.1017/S0373463317000698 Published online by Cambridge University Press

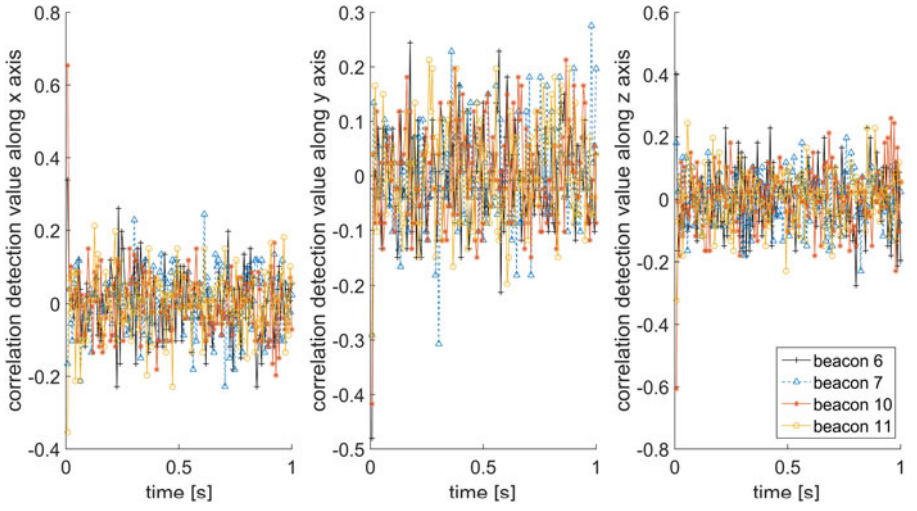

Figure 6. The correlation detection curves between the measurement sequences and each Gold code sequence from three orthogonal axes.

respectively, and two peaks along the x axis and z axis are higher than 0·6 in a period though the peak along the y axis is smaller than 0·5.The synchronisation between beacons and the sensor is successfully carried out according to the above regulation of distinguishing the initial position of the superposed encoded magnetic fields sequence.

After the time synchronisation, each beacon field can be estimated by solving Equation (13). On the one hand, the measurements mainly come from four beacons near the object and Earth's magnetic field. On the other hand, the location sequence consists of binary sequences, each bit has only two states, i.e. 1 and 0, thus, each bit of superposed encoded magnetic fields sequence is not more than 16 combinations, and their combinations are shown in Table 2. In this simulation, the four largest beacon field estimations are (0·0019, −0·0020, −0·0012), (0·0015, 0·0018, −0·0011), (−0·0015, −0·0013, −0·0011), (−0·0012, 0·0012, −0·0010), respectively, and the unit is Gauss. The fifth largest beacon field estimations are (0·1321, −0·0433, −0·2174), and the unit is mG. The process of positioning utilises only four beacon fields since the other beacons are too small to contribute to the measurements. As shown in Table 3, the first bit measurement sequence along the x axis is −0·007 G. In the first bit of 16 binary combination values along the x axis, the combination of minimum deviation between measurement and combination value is $(-1, -1, 1, 1, 1)$, which corresponds to $(0, 0, 1, 1, 1)$. Similarly, the deviations along the other axes correspond to this result. Thus, the real combination of the first bit superposition location sequence is obtained based on Equation (16), and the other bit of the superposition location sequence can be successively obtained by this method. Thus the location of the four beacons can be deduced.

Finally, the position of the object can be estimated by solving Equation (17) or Equation (19). If using the LM algorithm to separately solve Equation (17) along different axes, the results are (5·7467, 6·112, 1·6132), (5·7741, 6·1267, 1·6325), and (3·7003, 4·0088, 0·2119). According to the component of the magnetic field along the x,

https://doi.org/10.1017/S0373463317000698 Published online by Cambridge University Press

Table 2. The Configuration of Beacon location sequence and its superposed magnetic field.

	Results of binary combination form / G		
Binary combination form	x axis	y axis	z axis
(−1, −1, −1, −1, 1)	−0·0007	0·0004	0·0044
(−1, −1, −1, 1, 1)	−0·0032	0·0028	0·0024
(−1, −1, 1, −1, 1)	−0·0037	−0·0023	0·0022
(−1, −1, 1, 1, 1)	−0·0062	0·0001	0·0002
(−1, 1, −1, −1, 1)	0·0024	0·0039	0·0021
(−1, 1, −1, 1, 1)	−0·0001	0·0063	0·0001
(−1, 1, 1, −1, 1)	−0·0007	0·0013	0·0000
(−1, 1, 1, 1, 1)	−0·0032	0·0037	−0·0020
(1, −1, −1, −1, 1)	0·0032	−0·0037	0·0020
(1, −1, −1, 1, 1)	0·0007	−0·0013	0·0000
(1, −1, 1, −1, 1)	0·0001	−0·0063	−0·0001
(1, −1, 1, 1, 1)	−0·0024	−0·0039	−0·0021
(1, 1, −1, −1, 1)	0·0062	−0·0001	−0·0002
(1, 1, −1, 1, 1)	0·0037	0·0023	−0·0022
(1, 1, 1, −1, 1)	0·0032	−0·0028	−0·0024
(1, 1, 1, 1, 1)	0·0007	−0·0004	−0·0044

Table 3. The Measurements of Beacon Location Sequence Field.

Measurements of beacon location sequence field / G		
x axis	y axis	z axis
−0·0070	0·0001	0·0003
0·0058	−0·0001	−0·0002
−0·0007	0·0004	0·0063
−0·0007	0·0004	0·0063
0·0001	−0·0071	−0·0002
−0·0001	0·0059	0·0001
−0·0007	0·0004	0·0063
−0·0007	0·0004	0·0063
−0·0007	0·0004	0·0063
−0·0007	0·0004	0·0063
−0·0007	0·0004	0·0063
−0·0007	0·0004	0·0063

y, z axes, respectively, the corresponding Root Mean Square Errors (RMSE) are 24·06 cm, 25·06 cm and 180·35 cm. The results based on the z axis field are apparently not reliable.

The system error mainly comes from the bias of the beacon parameters, i.e., the loop current I, the number of turns n, the radius of coils a, and the location of the beacon. All of these parameters affect the magnitude of the magnetic dipole moment $\boldsymbol{M}$ except n, since n is established. In addition, if the length of the beacon location sequence is adequately long, the beacon location error would not affect the positioning result since the location data are derived from measurements rather than storing information. In this case, $|\boldsymbol{M}| \approx 58{\cdot}9049$, so the positioning results certainly have errors if I and a have some errors. The positioning errors caused by uncertainty of I and a are given in Figure 7. I and a vary from 1·5 to 4·5

https://doi.org/10.1017/S0373463317000698 Published online by Cambridge University Press

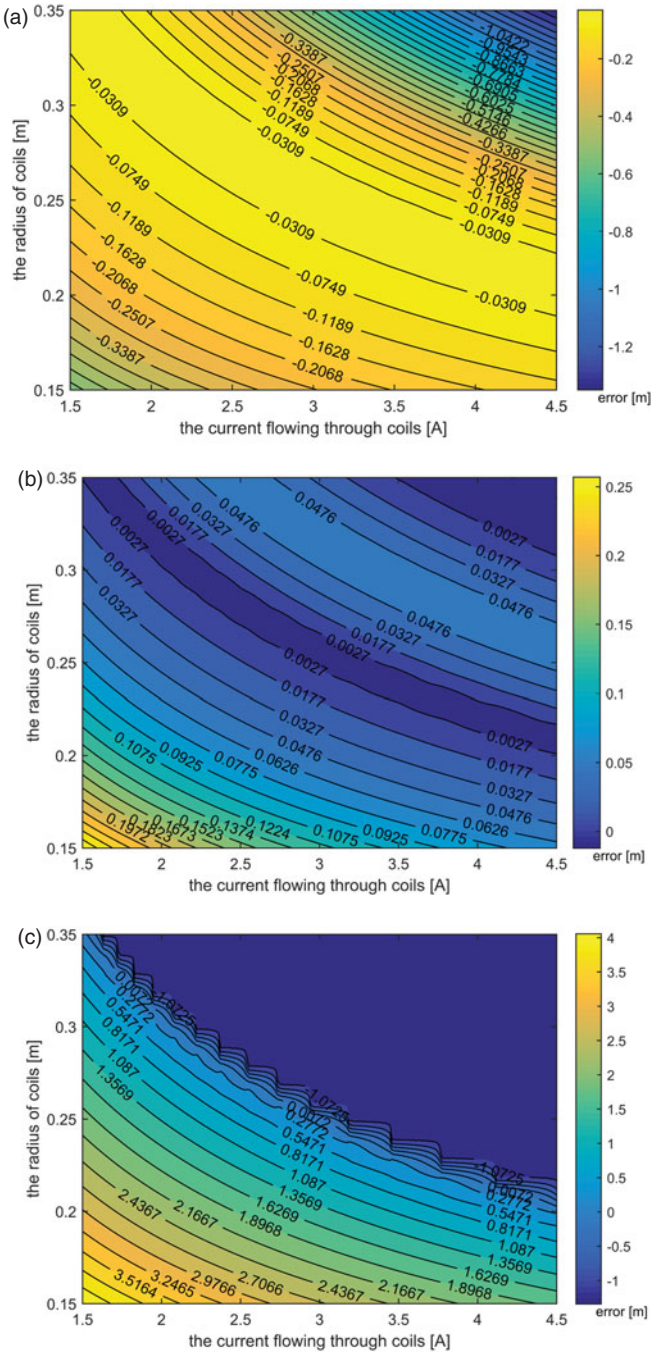

Figure 7. The positioning error respectively along (a) x, (b) y and (c) z axes caused by the bias of current and coils radius.

https://doi.org/10.1017/S0373463317000698 Published online by Cambridge University Press

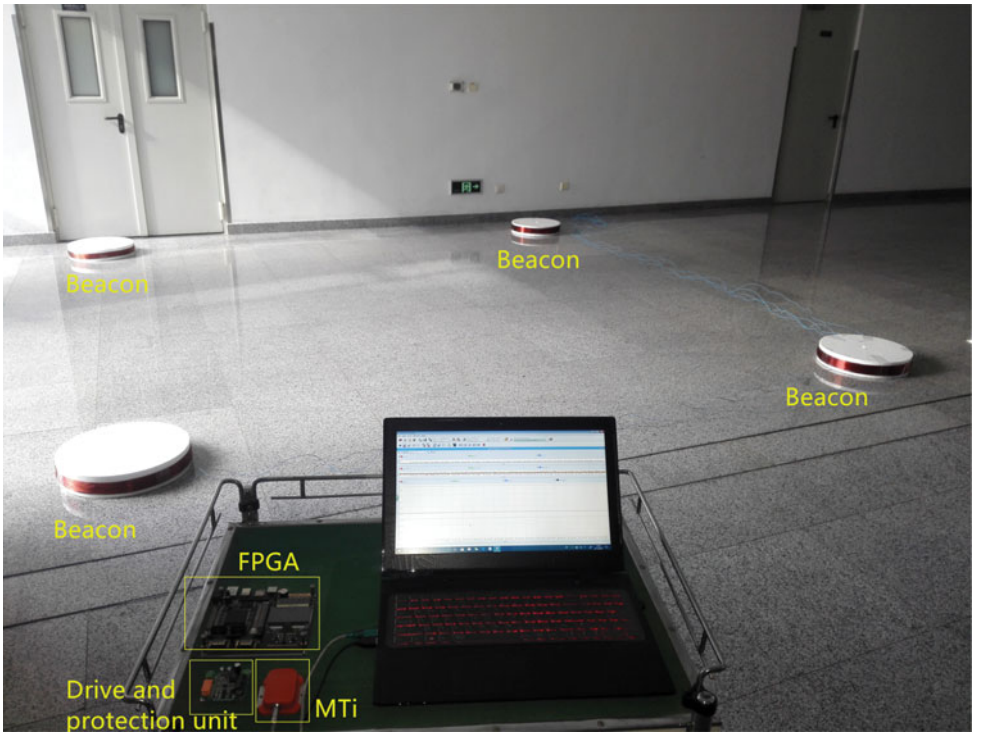

Figure 8. Four beacons comprised of coils are fixed in an indoor environment, and the sensor MTi is used for measuring the superposed encoded magnetic fields.

and 0·15 to 0·35, respectively. The variation range of $|\boldsymbol{M}|$ is consequently from 10·6029 to 173·1803. According to the positioning error along different axes, a small deviation of I and a, e.g. 20% deviation, would not result in the positioning results' invalidation. The positioning error along the z axis is about $-1{\cdot}2$ m if I and a continue to increase. Therefore, the positioning system can provide a reliable service.

5. PERFORMANCE VALIDATION OF POSITIONING SYSTEM. A prototype positioning system using artificial encoded magnetic fields was designed and tested in an indoor environment within a $4 \times 4 \times 3\,\mathrm{m}^3$ area. As shown in Figure 8, four beacons are located in a building-fixed coordinate frame, and their configuration is the same as the first four beacons in Table 1. Each beacon is comprised of circular coils with 100 turns, a coil radius of 0·25 m, and 4 A of current flowing through them. The test utilises a three-axis magnetometer which is embedded in a MTi Inertial Measurement Unit (IMU) from XSens, and some technical data with regard to the magnetometer can be seen in Table 4.

Figure 9 depicts the positioning system workflow. In accordance with the polarity of the current, the computer sets a unique Gold code sequence and location sequence for each beacon control unit. Afterwards, under the protection unit, the control unit and drive unit supply the current for the beacons in terms of assigned sequence. All beacons periodically create encoded magnetic fields at the same time; the object uses the magnetometer to measure the superposed magnetic field. Finally, the computer or mobile device solves the object

https://doi.org/10.1017/S0373463317000698 Published online by Cambridge University Press

Table 4. The Specification of Three-Axis Magnetometer in MTi.

Full range	+/− 750	[mG]
Linearity	0·2	[% of FS]
Bias stability	0·1	[mG 1σ]
Scale factor stability	0·5	[% 1σ]
Noise density	0·5 (1σ)	[mG /$\sqrt{}$Hz]
Alignment error	0·1	[deg]
Bandwidth	10	[Hz]
A/D resolution	16	[bits]

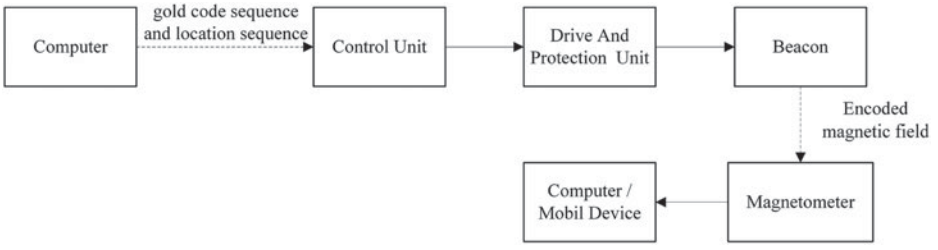

Figure 9. Schematic diagram of the positioning system using artificial encoded magnetic fields.

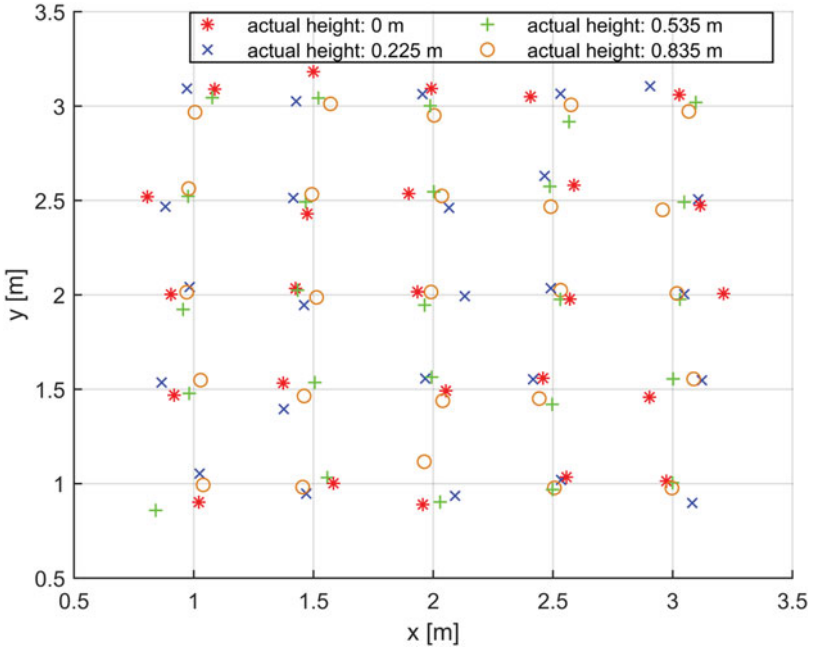

Figure 10. Horizontal position estimation in different heights.

position according to magnetic field measurements sent by the magnetometer. In the experiment, the control unit employs a development board with a Field Programmable Gate Array (FPGA), drive and protection units consisting of a voltage converter TP7660, switching

https://doi.org/10.1017/S0373463317000698 Published online by Cambridge University Press

voltage regulator LM2575 and an N-Channel enhancement mode power NCE80H11D. The FPGA simply provides the drive unit with high or low levels, which is sufficient to enable the beacon to create encoded magnetic fields. The update rate of the encoded magnetic fields' sequence is 2 Hz, and the sample rate of the sensors is 300 Hz. The driving voltage is 16 V, and the resistance of the coils is 4 Ω before working and increases to 4·5 Ω after a period of operation. Although the variation of resistance results in a change in the electrical current, current error of about 11% may not cause much of an impact on positioning based on the above simulation analysis. Consequently, the system does not give a feedback control for the current following through to the beacon.

The sensor is placed at four different heights, i.e., 0 cm, 22·5 cm, 53·5 cm, and 83·5 m and the interval is 50 cm along the x axis and y axis. Figure 10 shows the position estimation of the x direction and the y direction at the same height and the average bias errors along the x, y and z direction, which are 5·28 cm, 4·48 cm and 38·29 cm, respectively. The RMSE in these three directions are 6·80 cm 5·63 cm and 49·77 cm. While indoor positioning systems are more likely to focus on horizontal directional error, especially for mobile robot applications, the effect of vertical directional error is less important for the object. Therefore, the positioning system is effective.

6. CONCLUSION AND FUTURE WORK. In this paper, an indoor positioning system using artificial encoded magnetic fields has been presented. Encoded magnetic fields are periodically generated by multiple fixed and coplanar beacons, which are composed of uniaxial current carrying coils. The encoded magnetic field sequence of each beacon consists of a unique Gold code and beacon location sequence, and in both of them, 0 and 1 represent the direction of current. The Gold code has desirable properties of autocorrelation and cross-correlation in a CDMA structure, which can be used for time synchronisation and distinguishing the beacon field. A beacon location sequence, which is the binary code of the beacon location, lies at the end of the Gold code. Since the magnetic field signal provides information about time synchronisation and beacon location, it greatly enhances the availability of the positioning system. Furthermore, encoded magnetic fields are a kind of low frequency magnetic field, which can penetrate commonly used building materials without signal propagation error or multipath effects, and such a property is particularly suitable for indoor positioning.

The positioning process is divided into three steps. The first step is performing time synchronisation between the sensor and beacons according to correlation detection. The second step is to estimate the beacon field near the object and demodulate the beacon location. The last step is position estimation in accordance with the relation between the magnitude of the beacon field and distance. A simulation is performed to verify the positioning system, which shows that the system can provide available positioning even though there are some systematic errors. In addition, a prototype system has been developed to test its performance. The results show that 2D and 3D accuracy are at sub-decimetre and decimetre level, respectively.

In future work, the influence of two types of interference, i.e. ferromagnetic materials and eddy field noise, will be investigated. The various modulation schemes including FDMA for the beacon field will be implemented so that the beacon field can be fully exploited, rather than a weak beacon field signal that cannot be extracted from the Earth's magnetic field. Also, a low cost Inertial Measurement Unit (IMU), which is available in

almost all smart phones, will be integrated in the positioning system to improve the positioning update rate and enable the system to provide dynamic positioning results for a moving object. In addition, the attitude of the object will be analysed by combining IMU, the beacons' field and the Earth's magnetic field.

ACKNOWLEDGMENTS

The authors would like to thank Mr. Charndeep Bhangoo for his suggestions concerning the paper's use of English.

REFERENCES

Abrudan, T., Xiao, Z., Markham, A. and Trigoni, N. (2015). Distortion Rejecting Magneto-Inductive 3-D Localization (MagLoc). *IEEE Journal on Selected Areas in Communications*, **33**, 2404–2417.

Bernieri, A., Betta, G., Ferrigno, L. and Laracca, M. (2013). A novel biaxial probe implementing multifrequency excitation and SVM processing for NDT. *Proceedings of the 2013 IEEE International Instrumentation and Measurement Technology Conference (I2MTC), Minneapolis, Minnesota, USA.*

Blankenbach, J. and Norrdine, A. (2010). Position estimation using artificial generated magnetic fields. *Proceedings of the 2010 International Conference on Indoor Positioning and Indoor Navigation (IPIN), Switzerland.*

Blankenbach, J., Norrdine, A. and Hellmers, H. (2012). A robust and precise 3D indoor positioning system for harsh environments. *Proceedings of the 2012 International Conference on Indoor Positioning and Indoor Navigation (IPIN), Sydney, Australia.*

Hu, C., Li, M., Song, S., Yang, W.A., Zhang, R. and Meng, M. Q. H. (2010). A Cubic 3-Axis Magnetic Sensor Array for Wirelessly Tracking Magnet Position and Orientation. *IEEE Sensors Journal*, **10**, 903–913.

Kong, E.M.C., Kwon, D.W., Schweighart, S.A., Elias, L.M., Sedwick, R.J. and Miller, D.W. (2004). Electromagnetic formation flight for multisatellite arrays. *Journal of Spacecraft and Rockets*, **41**, 659–666.

Markley, F.L. (1987). Attitude determination using vector observations and the singular value decomposition. *Journal of the Astronautical Sciences*, **38**, 245–258.

Misra, P. and Enge, P. (2006). *Global Positioning System: Signals, Measurements and Performance Second Edition.* Lincoln, MA: Ganga-Jamuna Press.

Pasku, V., De Angelis, A., Dionigi, M., De Angelis, G., Moschitta, A. and Carbone, P. (2015). A Positioning System Based on Low Frequency Magnetic Fields. *IEEE Transactions on Industrial Electronics*, **63**, 2457–2468.

Prigge, E.A. (2004). *A positioning system with no line-of-sight restrictions for cluttered environments.* Stanford University.

Prigge, E.A. and How, J.P. (2004). Signal architecture for a distributed magnetic local positioning system. *IEEE Sensors Journal*, **4**, 864–873.

Pursley, M.B. (1977). Performance evaluation for phase-coded spread-spectrum multiple-access communication. i-system analysis. *IEEE Transactions on Communications*, **25**, 795–799.

Reitz, J.R., Milford, F.J. and Christy, R.W. (2008). *Foundations of Electromagnetic Theory (4th Edition)*. Addison-Wesley Publishing Company.

Sheinker, A., Ginzburg, B., Salomonski, N., Frumkis, L. and Kaplan, B.Z. (2013a). Localization in 2D Using Beacons of Low Frequency Magnetic Field. *IEEE Journal of Selected Topics in Applied Earth Observations and Remote Sensing*, **6**, 1020–1030.

Sheinker, A., Ginzburg, B., Salomonski, N., Frumkis, L. and Kaplan, B.Z. (2013b). Localization in 3-D Using Beacons of Low Frequency Magnetic Field. *IEEE Transactions on Instrumentation and Measurement*, **62**, 3194–3201.

Song, S., Hu, C., Li, M., Yang, W. and Meng, M.Q.H. (2009). Real time algorithm for magnet's localization in capsule endoscope. *Proceedings of the 2009 IEEE International Conference on Automation and Logistics, Shenyang, China.*